Rapid Communications

Loading of a continuous anion beam into a Penning trap with a view to laser cooling

G. Cerchiari, S. Erlewein,* C. König,† and A. Kellerbauer‡
Max Planck Institute for Nuclear Physics, Saupfercheckweg 1, 69117 Heidelberg, Germany

(Received 11 June 2018; published 14 August 2018)

The capture and confinement of a large and pure sample of anions into an ion trap is challenging due to the fragile nature of these weakly bound atomic systems. We present the results of an experimental study using Au^- in which anions from a keV-energy continuous beam were loaded into a cylindrical Penning trap. Experimental parameters such as stopping potential and axial trap depth were found to be crucial. The transfer of axial to radial momentum due to ion–ion collisions was identified as a main contributing factor to successful capture. A total number of up to 10^7 Au^- ions were loaded. The cooling of anions by simultaneously confined electrons was observed and seen to result in centrifugal separation of the two species. After storage times of several 10 s, electron cooling of the anions to the temperature of the cryogenic trap was achieved.

DOI: 10.1103/PhysRevA.98.021402

I. INTRODUCTION

Forty years after the first laser cooling of positive ions [1,2], this crucial technique has not yet been successfully applied to a negative ion species. Yet, the cooling of anions to ultracold temperatures would open up the possibility for precision measurements with anions that are not currently possible. For instance, certain molecules in the interstellar medium are only stable when they carry a negative charge. Their chemistry plays an important role in star formation [3].

We have been investigating the laser cooling of anions as a route towards the production of ultracold antihydrogen [4]. In this scheme, antihydrogen will be synthesized at approximately 100 mK by the charge exchange reaction of positronium with antiprotons sympathetically cooled by laser-cooled anions. Due to the large mass ratio of antiprotons to positrons, antihydrogen will be produced essentially at the antiprotons' temperature. Ultracold antihydrogen is a prerequisite for spectroscopic [5–7] and gravimetric [8–10] studies of antimatter at ultimate precision.

With a view to laser cooling, a very small number of atomic anions with fast (electric-dipole) transitions have been identified. We have been investigating the two most promising candidates, Os^- and La^-, by high-resolution laser spectroscopy in order to fully characterize the potential laser cooling transitions in these systems [11–14]. In our setup, the cooling transitions were probed by overlapping an excitation laser with an anion beam at a kinetic energy of a few keV from a Middleton-type Cs sputter ion source [15]. This type of source has been widely adopted for the production of anion beams from solid targets.

The extraction of negative ions from a sputter source using a high voltage has several advantages. Anions can be guided into regions with better vacuum conditions. Moreover, a kinetic energy of a few keV is practical for mass selection with a dipole magnet. For example, we have shown that in such a setup it is possible to separate elemental ^{139}La from its hydrides LaH, LaH_2, and LaH_4 [16]. The mass selectivity is crucial for laser cooling in a trap where the presence of contaminants would slow the cooling process.

As a next experimental step, efficient techniques to capture an anion beam into an ion trap must be established. This is challenging because the ions travel with a kinetic energy of a few keV, whereas their binding energy is of the order of 1 eV. The loading of (heavy) negative ions into a trap from a beam of keV energy has not been investigated previously. Instead, anions are typically produced *in situ* from a gas jet or by laser ablation. These techniques are, however, either not applicable to metallic species or lack the selectivity required to remove contaminants present in the target material.

In this article we present a technique for the deceleration, capture, and confinement of anions from a continuous beam in UHV conditions in a Penning trap. For these studies we used an Au^- beam (electron affinity $U_{EA} = 2.3$ eV) that can be easily produced at high currents (up to μA). The advantage of a Penning trap is the possibility to simultaneously confine heavy anions and electrons. The electrons, which quickly cool to the temperature of the surrounding trap by emitting synchrotron radiation, can thus efficiently cool the ions.

II. EXPERIMENTAL SETUP

Negative ions are produced by Cs sputtering from a solid target and extracted as a continuous beam with a kinetic energy between 0.5 and 2 keV. After the source, a 90-degree dipole magnet (radius 0.5 m, resolving power 180) selects the mass of interest. The cylindrical Penning trap is placed at a distance of about 2.5 m downstream of the dipole magnet. The trap electrodes are thermally connected to the first stage of the magnet's cryocooler and are thus cooled to <40 K.

The superconducting solenoid produces an axial magnetic field of up to $B = 6$ T in the trap region for radial confinement. A stack of 13 coaxial electrodes generates the electric field that

*Present address: CERN, 1211 Geneva 23, Switzerland.
†Present address: University of Heidelberg, Im Neuenheimer Feld 226, 69120 Heidelberg, Germany.
‡Corresponding author: a.kellerbauer@cern.ch

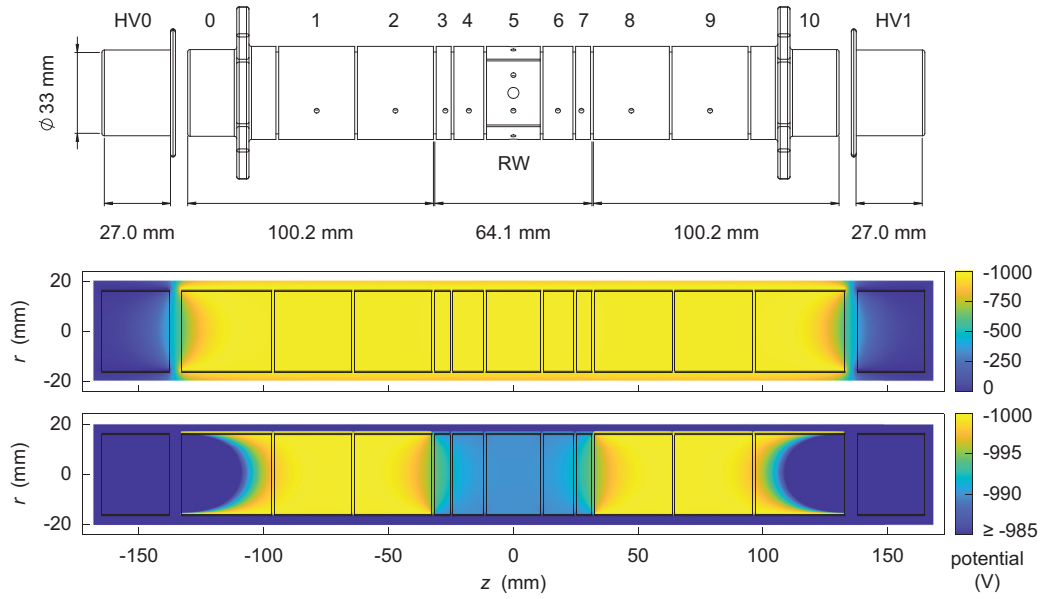

FIG. 1. (Top) Schematic drawing of the Penning trap electrodes. Electrode labels are indicated above; the beam direction is from left to right. Electrode 5 is split into four identical segments for rotating-wall (RW) excitation. (Bottom) False-color potential maps for a floating potential of −1000 V and a trap depth of 10 V in an axial section. The lower map is zoomed to the potential range from −985 to −1000 V.

constrains the axial ion motion. The geometry of the electrodes and the resulting potential are shown in Fig. 1. Three groups of electrodes are electrically connected to form the first end cap (100.2 mm), the central/ring section (64.1 mm), and the second end cap (100.2 mm). Electrode HV0 is connected to ground potential. Ions enter the trap through electrode HV0.

To create a trap for negative particles, the central section is kept at a higher potential with respect to the end caps. The axial potential is thus defined by three potentials designated *front, center*, and *rear* (in beam direction). The power supplies that provide these voltages are located on a high-voltage platform biased with a common *floating* potential. In the experiments reported here, the rear end cap potential was kept at an equal or higher absolute value than the front end cap to prevent ion loss in the downstream direction.

The *stopping potential* is defined as the sum of the front and the floating potential, since this corresponds to the kinetic energy that charged particles must have in order to enter the trap region. The term *trap depth* designates the difference between the ring and front end cap potentials. Each end cap can be switched between two potentials within 50–100 ns, thus modifying the axial potential to release particles in either direction.

An imaging microchannel plate (MCP) detector (diameter 40 mm) is mounted downstream at a distance of 280 mm from the trap center. The detector's phosphor screen is monitored with a digital camera (Allied Vision Mako) to record the ejected ions. The magnetic-field intensity at the front face of the detector is about eight times weaker than in the trap center. Hence the ions' radial position on the detector is magnified by a factor $\sqrt{8}$.

III. EXPERIMENTAL RESULTS

A. Trapping only anions

Anion capture in the trap was achieved by continuously streaming the ion beam into the trapping region and allowing the trap to fill gradually. The loading process was started and stopped by switching the potential of an electrode upstream of the dipole magnet, which can vary the trap loading time by selectively deflecting the ion beam. The beam alignment was found to be critical for successful trapping. Proper alignment was ensured by optimizing the transmission through the trap while raising the stopping potential near the accelerating potential (and hence the beam energy).

After beam alignment, a central well was prepared with a potential more positive than the front and rear potentials. The floating potential was set equal to the acceleration voltage. The front potential was set to +5 V and the rear potential (which reflects the ions) to values from −100 V to −120 V in all measurements reported here. The stopping barrier was then varied by changing the floating potential.

Incoming anions strongly decelerate between electrode HV0 and electrode 0. In the trap region, deflection of the ions transfers momentum from the axial to the radial direction, thus reducing the axial kinetic energy and preventing them from escaping towards the entrance. Several possible deflection mechanisms may occur, including anion–anion elastic or inelastic (detachment) scattering, or interaction with the residual gas.

In order to find suitable conditions for anion capture, we performed trapping trials for several combinations of stopping potential and trap depth. A two-dimensional false-color plot of these parameters is shown in Fig. 2. The stopping potential proved to be critical. It had to be set a few volts below the accelerating potential, such that anions remain trapped if their axial energy is reduced by just a few eV due to energy transfer to the radial direction. The optimal stopping potential was always found to be 2–7 V below the accelerating voltage, regardless of its absolute value.

The trap depth determines the ions' kinetic energy in the trap center. As shown in Fig. 2, its optimal value typically ranged

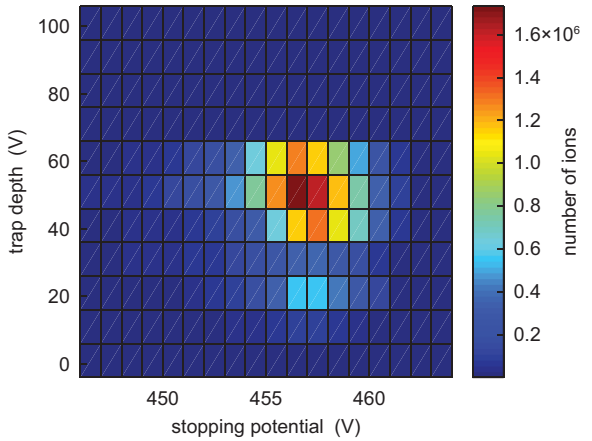

FIG. 2. Number of trapped ions (color code) as a function of stopping potential and trap depth. The loading time was 20 s, the magnetic-field magnitude 2 T, the beam energy −458 eV.

in the tens of volts. At a higher trap depth, scattering events are likely to transfer more kinetic energy to the radial component of the motion. However, the magnetic-field confinement limits the radial amplitude, which must not exceed the electrode inner radius of 16.5 mm.

In addition, suboptimal collimation of the incoming beam and the electrostatic focusing at the trap entrance cause an initial radial motion which compounds the limitation of radial confinement. As expected, we observed an increase of the optimal trap depth value with increasing magnetic field, as shown in Fig. 3. Using the linear trend observable in the figure, we find that the cyclotron radius of an Au^- ion at the optimal trap depth is $r_c \approx 11$ mm, regardless of the magnetic-field magnitude.

B. Trapping anions with electrons

In the presence of a cooling mechanism, trapping is expected to become more efficient because capture is achieved not only by momentum transfer due to scattering, but also by a net reduction in kinetic energy. Compared to linear radiofrequency traps [17], Penning traps offer the advantage of simultaneously confining anions along with electrons that may act as a cooling medium.

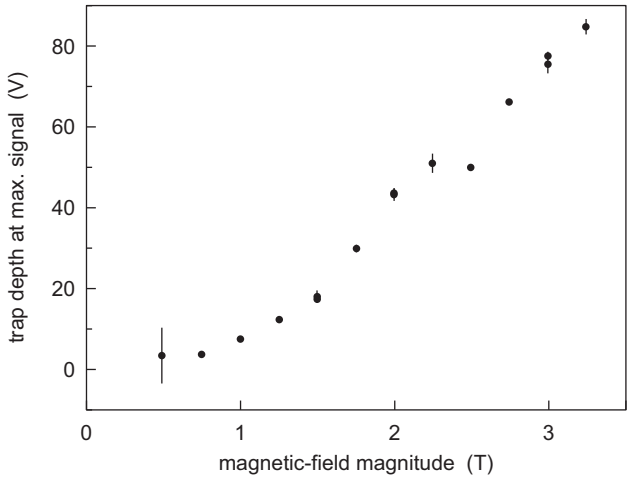

FIG. 3. Optimal trap depth as a function of magnetic-field magnitude. Some data points above $B = 3.5$ T had to be excluded due to a malfunction of the magnet power supply.

Electrons are readily produced in large quantities by a hot cathode. In our apparatus, an electron gun can be inserted into the beam line upstream of the trap. In the strong magnetic field of the Penning trap, electrons lose kinetic energy by emitting synchrotron radiation. The dissipated power per unit time is given by Larmor's formula for an accelerated nonrelativistic ion [18]. It follows that the kinetic energy decreases exponentially with a characteristic time constant [19],

$$\tau = \frac{3\pi\epsilon_0 m_e^3 c^3}{e^4 B^2}. \tag{1}$$

In a 5-T magnetic field the time constant is $\tau = 0.1$ s, which ensures that thermalization of electrons with the surrounding environment occurs within about 1 s, reaching equilibrium with the black-body radiation of the trap at $T < 40$ K. Electrons can, therefore, constitute a buffer medium that cools other negatively charged particles via Coulomb interactions without adversely affecting the vacuum.

The considerable difference in the number of stored e^- and anions (2 or more orders of magnitude) made it necessary to separate the two species before the destructive measurement on the MCP. The mass difference of the two species can be exploited for separation [20]. A short (500 ns) pulse on the front end cap proved to be sufficient to expel electrons from the trap towards the direction opposite from the detector, while preserving the more massive anions inside the central section.

Thus it was possible to apply higher voltages and amplification gain to the MCP for anion detection, reaching near-single-particle sensitivity. On the other hand, if anions and electrons radially overlap prior to electron ejection, collisions occur between them as the e^- are accelerated outward. These collisions may lead to anion neutralization, thus reducing the number of detected particles. We estimate that the effect could in some instances lead to a reduction in the number of detected anions by a factor two.

The trap was preloaded with about 2.2–2.4 $\times 10^9$ electrons (density $n \approx 1$–5×10^7 mm^{-3}) and subsequently floated to the stopping potential. The number of trapped Au^- ions from a 5(1) nA beam was then measured as a function of stopping potential and trap depth both with and without electrons, as shown in Fig. 4. The number of trapped anions was recorded as a function of the two potentials, with the other parameter held fixed at its optimal value. These optimal values were found not to remain constant as the second parameter was scanned.

The optimal value for the stopping potential with e^- was found to be slightly lower than without (≈0 V versus ≈5 V, relative to the beam energy). Conversely, for constant stopping potential the optimal trap depth was found to be larger with e^- than without (≈50 V versus ≈40 V). Both effects are easily understood by the effect of the electron plasma's space charge, which counteracts externally applied potentials. In the presence of electrons, the trapping efficiency also becomes more sensitive to the stopping potential.

The trapping efficiency then exhibits an additional narrower peak which is centered near zero stopping potential (again,

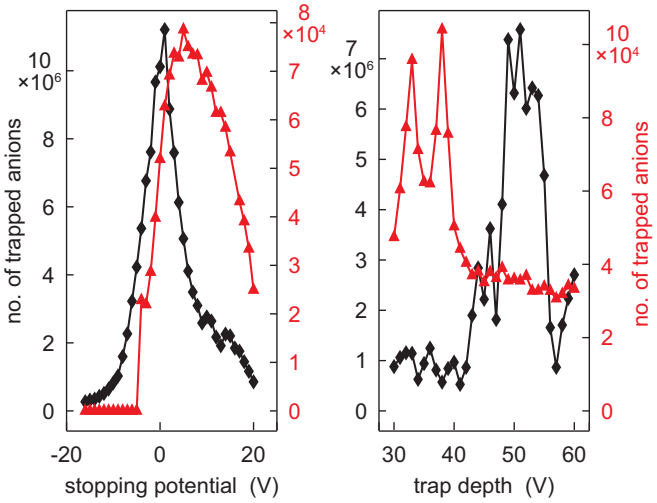

FIG. 4. Number of trapped anions with (black diamonds, left scale) and without electrons (red triangles, right scale) as a function of the stopping potential (left pane, relative to the acceleration voltage of 1008 V) and the trap depth (right pane). The other parameter was held fixed at its optimal value. Solid lines are meant to guide the eye. Error bars are smaller than the symbols.

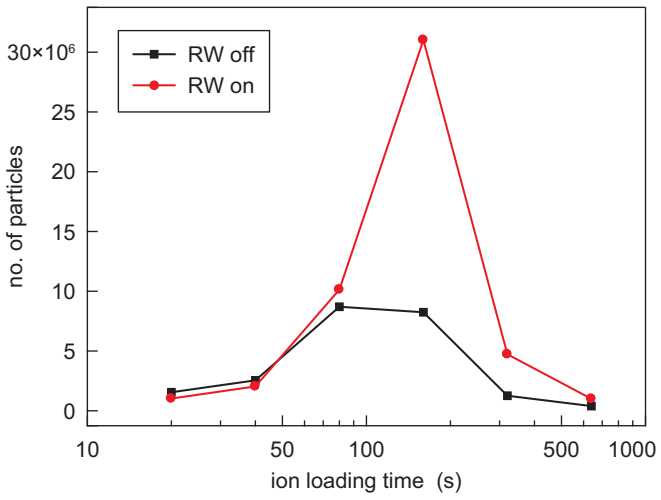

FIG. 5. Number of anions as a function of loading time with RW excitation off (black squares) and on (red circles). The RW frequency was 3 MHz, the amplitude 120 mV (peak-to-peak). Solid lines are meant to guide the eye.

relative to the beam energy). This is likely due to the fact that the viscous drag created by the electron plasma exerts only a very weak axial force on the incoming anions. In order to stop them in one passage, the beam energy must be near zero. Moreover, a larger beam energy may cause collisional detachment. Most importantly, as shown in Fig. 4, the presence of electrons increases the number of trapped anions by about two orders of magnitude for the same loading time (20 s).

For longer loading times the process tends to lose efficiency. As the e^- plasma expands within several 10 s, its density decreases and anions are dragged along towards the trap wall and lost. A well-established technique to counteract this expansion is the application of a torque to the stored e^- plasma by rotating-wall (RW) excitation [21]. With the correct drive parameters, the radius of the electron cloud can be reduced continuously or at regular intervals, thus preserving the electron plasma for longer times and extending the loading time.

In our operating conditions, the radial shape of the e^- plasma was preserved using an RW drive at a frequency of 3 MHz and an amplitude of 120 mV. We performed a set of loading trials with ≈50 V center potential and the stopping potential optimized for anion capture. The results with and without RW excitation are shown in Fig. 5. For the first ≈60–80 s of loading, we observe a comparable efficiency with and without RW excitation. About 8×10^6 anions were trapped in both conditions because the e^- plasma expansion has not yet become detrimental to the loading process. After 160 s, up to 2.9×10^7 anions were trapped with RW excitation. Conversely, the number of anions loaded without RW excitation did not further increase beyond 10^7 even after longer loading times.

Anion losses for very long loading times are caused by a slow e^- plasma expansion. The expanding electrons drag the already captured anions against the trap walls, where they are lost. The expansion occurs despite continuous RW excitation due to an inevitable deviation from the optimal RW amplitude and frequency that would ensure indefinite plasma stability. In addition, any change in electron density also affects the optimal trapping parameters (Fig. 4), thus reducing the capture efficiency with reduced electron number and density.

C. Sympathetic cooling of anions by electrons

The sympathetic cooling effect of the electrons can be further exploited to prepare anions for laser cooling. Reducing the initial temperature of the trapped sample to a few K may help alleviate the limitation caused by the relatively low scattering rate of atomic transitions in negative ions. As the mixed plasma thermalizes, the two species tend to occupy different radial regions in the trap due to their mass difference (centrifugal separation [22]). After complete separation the interaction between electrons and anions is strongly reduced and the anions have reached the lowest temperature achievable by electron cooling.

In thermal equilibrium at temperature T the probability p to find an anion with charge q and mass m at a distance r from the axis follows the Maxwell-Boltzmann distribution [23]:

$$p \propto \exp\left(\frac{q}{k_B T}\left(\phi(r) - \frac{m\omega_r^2 r^2}{2q} - \frac{B\omega_r r^2}{2}\right)\right), \qquad (2)$$

where ϕ is the space charge potential, ω_r the ion's angular velocity around the trap axis, and k_B the Boltzmann constant. Conversely, the electron distribution is, in general, similar to a step function and can be approximated as uniform up to a cut-off radius. In this approximation the plasma edge is sharp, and the electric potential ϕ is proportional to r within the plasma.

The plasma dynamics is approximated by a rigid rotation around the axis at constant angular velocity ω_r, which is proportional to the plasma density n_0 [24]. We calculated n_0 from the particle density near the axis measured when releasing both species onto the MCP. The model allows fitting the radial anion distribution using Eq. (2) in order to

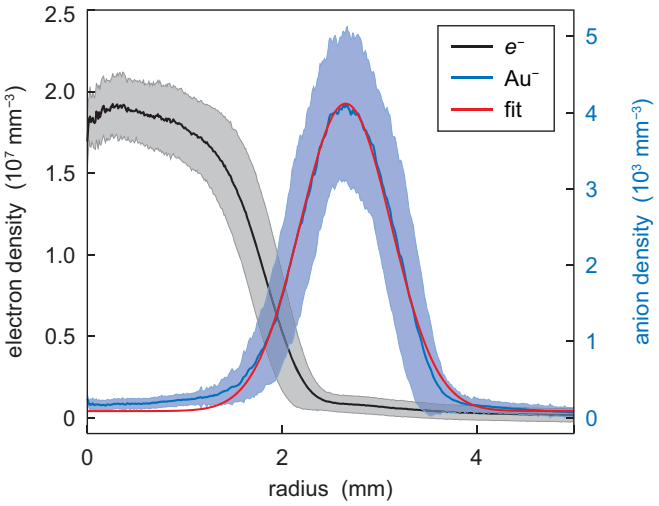

FIG. 6. Radial density of e^- (black line, left scale) and anions (blue line, right scale) at 351 s after anion loading. The shaded areas represent 1-σ uncertainties. The fit of the anion distribution with a Maxwell-Boltzmann distribution is indicated by the solid red line.

extract the temperature, as shown in Fig. 6. This technique for calculating the temperature is based on the change of the anion cloud's shape and is, therefore, primarily applicable during the centrifugal-separation phase at low temperature, while it suffers from a lack of sensitivity in the high-temperature regime. Using this technique, we determined an asymptotic anion temperature of 15(6) K.

To estimate the cooling time scale in our experimental setup, we performed loading trials with an anion loading time of 5 s without RW excitation, as shown in Fig. 7. We observed centrifugal separation between the two species after 250 s of storage time and fitted the data acquired during the phase transition to provide an additional estimate of the final anion temperature. The centrifugal separation was identified

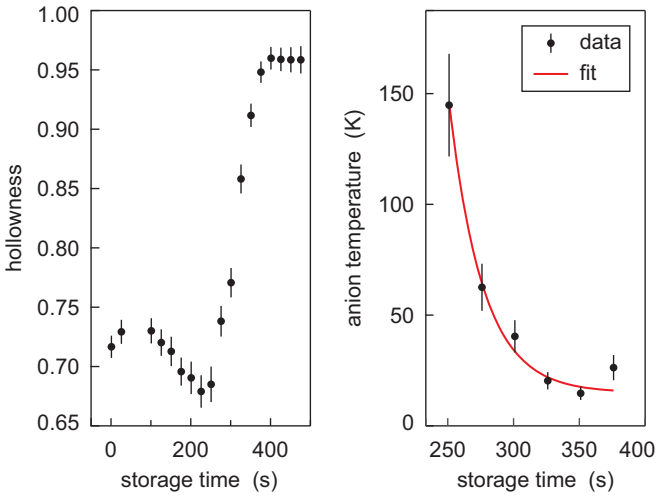

FIG. 7. (Left pane) Hollowness (see definition in the text) as a function of storage time. (Right pane) Anion temperature during centrifugal separation. The exponential fit (solid red line) yields a time constant of 25.5(9.0) s and an asymptotic temperature of 15(6) K.

by calculating the hollowness of the acquired images. This parameter has been used in the context of mixed plasmas in Ref. [25]. It is defined as $H = \langle r^2 \rangle^{1/2} \cdot \langle r^4 \rangle^{-1/4}$, where brackets denote the spatial average over the radial profile. The hollowness is $H = 1$ for a thin annulus and is lower for a distribution with higher central density.

Our analysis suggests that the separation of the two species occurs between 250 s and 380 s storage time. Anions are cooled to a temperature of 18(7) K after ≈350 s, which is compatible with the temperature of the trap electrodes, with a time constant of about 30 s. This cooling time scale is comparable with previous measurements using electrons and Au^- ions [26]. The extrapolated initial anion temperature (at time $t = 0$) is $k_B T = 210(730)$ eV. This is roughly similar to the trap depth, which, in turn, determines the residual energy of the anions after capture. The large uncertainty stems from the technique used for determining the anion temperature, which is mostly sensitive at low temperature.

A more accurate model for thermalization has been proposed by Spitzer [27]. Disregarding the self-cooling of the electrons, the energy dissipation follows an exponential decay with time constant,

$$\theta(m) \propto m\left(\frac{k_b T}{mc^2} + \frac{k_b T_e}{m_e c^2}\right)^{\frac{3}{2}}. \tag{3}$$

Due to the large mass ratio between anion and electrons, the term $k_b T/(mc^2)$ can be neglected at low temperature. Hence the cooling times for different anions in similar conditions should scale with their mass. Considering the time scale of centrifugal separation (from hollowing to final state) of 60 ms for antiprotons [25], a separation time of more than 10 s for Au^- should be expected. Thus, we can deduce that electron cooling of La^- in our system should occur with a time constant well below 20 s.

IV. CONCLUSION

In this work, we presented a trapping method to load anions into a Penning trap from a continuous keV-energy beam. In capturing ions, the trap was biased to a high voltage to reduce the kinetic energy of the incoming ions from some keV to a few eV. Anion trapping was realized in a fully static trap configuration thanks to a reduction of the ions' axial momentum component due to scattering processes.

We find that the capture efficiency can be enhanced by two orders of magnitude by preloading an electron plasma into the trap. Finally, we show that electrons constitute an efficient buffer cooling medium that can reduce the anion temperature to a few tens of K within a few tens of seconds of storage time. From the outcome of our analysis we deduce that electron cooling of La^- should occur within 250 s after loading.

ACKNOWLEDGMENTS

We thank the MPIK accelerator group and workshop for invaluable assistance with the ion source and R. Caravita (CERN) for helpful discussions. This work was supported by the European Research Council (ERC) under Grant No. 259209 (UNIC).

[1] D. J. Wineland, R. E. Drullinger, and F. L. Walls, Phys. Rev. Lett. **40**, 1639 (1978).
[2] W. Neuhauser, M. Hohenstatt, P. Toschek, and H. Dehmelt, Phys. Rev. Lett. **41**, 233 (1978).
[3] M. A. Cordiner, J. V. Buckle, E. S. Wirström, A. O. H. Olofsson, and S. B. Charnley, Astrophys. J. **770**, 48 (2013).
[4] A. Kellerbauer and J. Walz, New J. Phys. **8**, 45 (2006).
[5] C. L. Cesar *et al.* (ALPHA Collaboration), Can. J. Phys. **87**, 791 (2009).
[6] G. Gabrielse *et al.* (ATRAP Collaboration), Phys. Rev. Lett. **100**, 113001 (2008).
[7] N. Kuroda *et al.* (ASACUSA Collaboration), Nat. Commun. **5**, 3089 (2014).
[8] A. Kellerbauer *et al.* (AEGIS Proto-Collaboration), Nucl. Instrum. Methods B **266**, 351 (2008).
[9] M. Doser *et al.* (AEGIS Collaboration), Classical Quantum Gravity **29**, 184009 (2012).
[10] P. Indelicato *et al.* (GBAR Collaboration), Hyperfine Interact. **228**, 141 (2014).
[11] U. Warring *et al.*, Phys. Rev. Lett. **102**, 043001 (2009).
[12] A. Kellerbauer, A. Fischer, and U. Warring, Phys. Rev. A **89**, 043430 (2014).
[13] E. Jordan, G. Cerchiari, S. Fritzsche, and A. Kellerbauer, Phys. Rev. Lett. **115**, 113001 (2015).
[14] G. Cerchiari, A. Kellerbauer, M. S. Safronova, U. I. Safronova, and P. Yzombard, Phys. Rev. Lett. **120**, 133205 (2018).
[15] R. Middleton, Nucl. Instrum. Methods **214**, 139 (1983).
[16] A. Kellerbauer, G. Cerchiari, E. Jordan, and C. W. Walter, Phys. Scr. **90**, 054014 (2015).
[17] F. Herfurth *et al.* (ISOLTRAP Collaboration), Nucl. Instrum. Methods B **469**, 254 (2001).
[18] J. D. Jackson, *Classical Electrodynamics* (Wiley, New York, 1999).
[19] L. S. Brown and G. Gabrielse, Rev. Mod. Phys. **58**, 233 (1986).
[20] L. Suess, Y. Liu, and F. B. Dunning, Rev. Sci. Instrum. **76**, 026116 (2005).
[21] F. Anderegg, E. M. Hollmann, and C. F. Driscoll, Phys. Rev. Lett. **81**, 4875 (1998).
[22] T. M. O'Neil, Phys. Fluids **24**, 1447 (1981).
[23] F. Anderegg, *Rotating Wall Technique and Centrifugal Separation* (World Scientific, Singapore, 2016).
[24] D. H. E. Dubin, AIP Conf. Proc. **1521**, 26 (2013).
[25] G. B. Andresen *et al.* (ALPHA Collaboration), Phys. Rev. Lett. **106**, 145001 (2011).
[26] G.-Z. Li, S. Guan, and A. G. Marshall, J. Am. Soc. Mass Spectrom. **8**, 793 (1997).
[27] L. Spitzer, *Physics of Fully Ionized Gases*, 2nd revised ed. (Dover, Mineola, 2013).